Smart Mater. Struct. 7 (1998) 237–247. Printed in the UK

PII: S0964-1726(98)90527-4

Tunable laser demodulation of various fiber Bragg grating sensing modalities

R M Measures, M M Ohn, S Y Huang, J Bigue and N Y Fan

Fiber Optic Smart Structures Laboratory, University of Toronto Institute for Aerospace Studies, 4925 Dufferin Street, North York, M3H 5T6, Ontario, Canada

Received 20 January 1997, accepted for publication 12 June 1997

Abstract. Fiber optic Bragg grating technology offers unrivaled sensing versatility combined with the promise of extremely compact, rugged and low-cost integrated optoelectronic microchip demodulation systems. We show that a tunable laser can be used to demodulate each of the different sensing modalities: short and long gage fiber optic strain sensors; serial and parallel multiplexed fiber grating sensor arrays and truly distributed sensing based on intragrating strain profile mapping. We also show that distributed strain sensing is not limited by the length of a single Bragg grating. We demonstrate that Fourier transform analysis combined with tunable laser interrogation of a string of gratings permits distributed sensing over distances of about a meter without the need for high-cost time division multiplexing or producing each grating with a different reference wavelength as required by wavelength division multiplexing.

1. Introduction

The diversity of structural sensing possible with fiber optic Bragg grating technology includes short and long gage length fiber optic strain sensors, serial and parallel multiplexed fiber grating sensor arrays and distributed sensing that can map strain profiles. Furthermore, the use of fiber Bragg gratings permits strain measurements to be made over an extended period of time, and allows transient stress events to be captured. The intrinsic very high frequency response of this type of sensor makes it possible to detect acoustic emission or undertake acoustic sounding. The ease with which these fiber optic sensors are embedded within composite materials, as well as adhered to the surface of structures, could allow them to play a significant role in speeding the introduction of advanced composite materials to bridges and other structures by providing a built-in monitoring capability. Smart repair and strengthening of structures as diverse as bridges and aircraft are also possible with such fiber optic structurally integrated sensing systems.

In the past the diverse sensing modalities (short and long gage; multiplexed and distributed) possible with fiber Bragg grating (FBG) technology have led to a number of different methods of sensor demodulation (Kersey *et al* 1992, 1993, Measures *et al* 1992, Fan *et al* 1997). In this paper we show that each of these sensing modalities can be demodulated with a tunable laser. Short gage length FBG sensors will not be treated separately in this paper, for clearly any system that can interrogate a linear array of such sensors can also demodulate a single sensor. We shall show how a tunable laser can be used to interrogate a long gage strain sensor that is localized by a fiber Bragg grating to form a sensing Fabry–Pérot interferometer of arbitrary gage length within an optical fiber.

We shall also introduce a new technique based on Fourier transform analysis that permits, for the first time, the measurement of strain profiles that are not restricted to being monotonic or the use of a single fiber Bragg grating. In this approach both the intensity and phase spectra reflected from either an extended single FBG sensor, or a linear array of gratings, as a tunable laser scans a predetermined spectral interval, are used to derive the strain profile (Huang *et al* 1997).

For applications requiring a string of Bragg grating sensors along a length of optical fiber, wavelength division multiplexing (WDM) can be employed. This is possible because each grating can have a different reference wavelength so if the separation between the reference wavelengths is greater than the largest strain induced wavelength shifts likely to be encountered there will be no ambiguity in measuring the wavelength of each grating as this will indicate both its strain and which grating it is in the string. Recently, Nellen *et al* (1997) have demonstrated a serially wavelength multiplexed fiber Bragg gratings strain measuring system for use with concrete cantilever beams and carbon fiber cables to be used in a cabled stay bridge. They used an array of seven FBG sensors that were inscribed directly in the optical fiber during its manufacture.

In the case of WDM, the spectral bandwidth of the source limits the number of sensors, and the spatial resolution is limited by the length of fiber in which this

0964-1726/98/020237+11$19.50

number of sensors can be placed. With current light sources (having a typical spectral width of 100 nm) and a desired strain range of 5000 $\mu\varepsilon$ (or ~6 nm), about 15 such sensors can be WDM. If a larger number of sensors are to be interrogated then time division multiplexing (TDM) can be employed. In this approach short duration light pulses are used to determine which grating is being interrogated by means of a time of flight measurement. In TDM the number of sensors and their spatial resolution tend to be limited by cost. The higher the spatial resolution required, the shorter the pulse and the faster the processing optoelectronics. Optical power budget considerations can also limit the number of gratings that can be serially interrogated by this means.

In this paper we show that the same kind of tunable laser technique that can be used for distributed strain sensors with a single grating sensor can also be used for interrogating a string of grating sensors along an optical fiber, even though the laser's tuning range is far less than required for WDM and it is not pulsed, as required for TDM. As with the distributed sensing case this new approach requires that both the reflected intensity and the phase of the optical signal returned from the linear array of gratings be measured as a function of laser wavelength. Fourier transform analysis then provides the strain and grating location information for each of the grating sensors in the string. Unfortunately, for multiplexed arrays extending more than a meter or so the frequencies involved in the Fourier spectrum become very high and impractical. For these situations we show that a tunable laser combined with Fourier transform analysis can still be used to identify pairs of fiber Bragg gratings that are strained relative to their neighbours. Lastly, it follows that if there is sufficient power in the laser it is also possible to undertake both serial and parallel multiplexing.

2. Distributed strain sensing based on Fourier transform methods

At any location within a single-mode optical fiber containing a Bragg grating there exist two waves: a forward wave with a complex amplitude, $F(z)$, and a backward wave with a complex amplitude, $B(z)$. Kogelnik (1976) has shown that the relation between these waves for a chirped grating can be given in terms of the grating reflection coefficient

$$r(z) = B(z)/F(z) \tag{1}$$

by the first-order differential equation

$$\frac{\mathrm{d}r(z)}{\mathrm{d}z} = \mathrm{i}\kappa(z)\left[\exp\left\{-\mathrm{i}\left[2z\Delta\beta(z) - \phi(z)\right]\right\} + r(z)^2\exp\left\{\mathrm{i}\left[2z\Delta\beta(z) - \phi(z)\right]\right\}\right] \tag{2}$$

where $\kappa(z)$ is the coupling coefficient for the grating (real variable), $\phi(z)$ is the incremental grating phase due to perturbations, and $\Delta\beta(z)$ is the deviation in the propagation constant from the unperturbed Bragg wavelength, i.e.

$$\Delta\beta(z) = \beta(z) - \pi/\Lambda_0. \tag{3}$$

Here $\beta(z)$ is the propagation constant at location z and Λ_0 is the unperturbed grating period. Kogelnik's definition of the incremental grating phase $\phi(z)$ is the phaseshift arising from the accumulated changes in the period of the grating, between $z = 0$ and $z = z$, relative to the unperturbed state and leads to the relation

$$\phi(z) = -\int_{z=0}^{z}\frac{2\pi}{\Lambda_0}\frac{\Delta\lambda(z)}{\lambda_0}\,\mathrm{d}z = -\frac{2\pi}{\Lambda_0}\int_{z=0}^{z}G_f\varepsilon(z)\,\mathrm{d}z \tag{4}$$

where $z = 0$ corresponds to the grating end closest to the source. For the case of non-uniform strain induced perturbations this must be generalized to account for the strain optic effect, leading to the more general relation

$$\phi(z) = -\int_{z=0}^{z}\frac{2\pi}{\Lambda_0}\frac{\Delta\Lambda(z)}{\Lambda_0}\,\mathrm{d}z \tag{5}$$

where the grating gage factor

$$G_f = 1 - n_0^2\left[p_{12} - \nu\left(p_{11} + p_{12}\right)\right]/2 \tag{6}$$

and $\varepsilon(z)$ is the local strain in the grating. p_{11} and p_{12} are the strain optic constants for the optical fiber.

For a low-reflectivity grating $|B(z)/F(z)| \ll 1$, and the second term in equation (2) can be neglected. This permits the equation to be integrated along the Bragg grating to yield

$$r(L) - r(0) = \mathrm{i}\int_{z=0}^{z=L}\left(\kappa(z)\mathrm{e}^{\mathrm{i}\phi(z)}\right)\mathrm{e}^{-\mathrm{i}(2z\Delta\beta)}\,\mathrm{d}z \tag{7}$$

where $z = L$ corresponds to the end of the grating furthest from the source. Since we can assume $r(L) = 0$, as $B(L) = 0$, and the complex reflection coefficient is also a function of $\Delta\beta$, equation (7) takes the form

$$r(\Delta\beta) = -\mathrm{i}\int_{z=0}^{z=L}\left(\kappa(z)\,\mathrm{e}^{\mathrm{i}\phi(z)}\right)\mathrm{e}^{-\mathrm{i}(2z\Delta\beta)}\,\mathrm{d}z \tag{8}$$

where we have used $r(\Delta\beta)$ to represent $r(z = 0, \Delta\beta)$. Equation (8) shows that $r(\Delta\beta)$ is the Fourier transform of the complex coupling coefficient $\kappa(z)\,\mathrm{e}^{\mathrm{i}\phi(z)}$.

In this case the inverse Fourier transform takes the form

$$\kappa(z)\,\mathrm{e}^{\mathrm{i}\phi(z)} = \frac{\mathrm{i}}{\pi}\int_{-\infty}^{\infty}r(\Delta\beta)\,\mathrm{e}^{\mathrm{i}2z\Delta\beta}\,\mathrm{d}(\Delta\beta). \tag{9}$$

The complex reflection coefficient is, of course, also a function of wavelength as

$$\Delta\beta(z) = \frac{2\pi n(z)}{\lambda(z)} - \frac{2\pi n_0}{\lambda_0} \approx -\frac{2\pi n_0}{\lambda_0^2}\Delta\lambda \tag{10}$$

with $\Delta\lambda = \lambda(z) - \lambda_0$ and λ_0 being the Bragg wavelength for the unperturbed grating. We assume that the deviations in n and λ produced by the perturbations are quite small. The complex reflection coefficient can also be expressed in the form

$$r(\Delta\lambda) = \sqrt{R(\Delta\lambda)}\,\mathrm{e}^{-\mathrm{i}\psi(\Delta\lambda)} \tag{11}$$

where $R(\Delta\lambda)$ and $\psi(\Delta\lambda)$ represent the intensity and phase spectra, respectively, for the grating measured at $z = 0$.

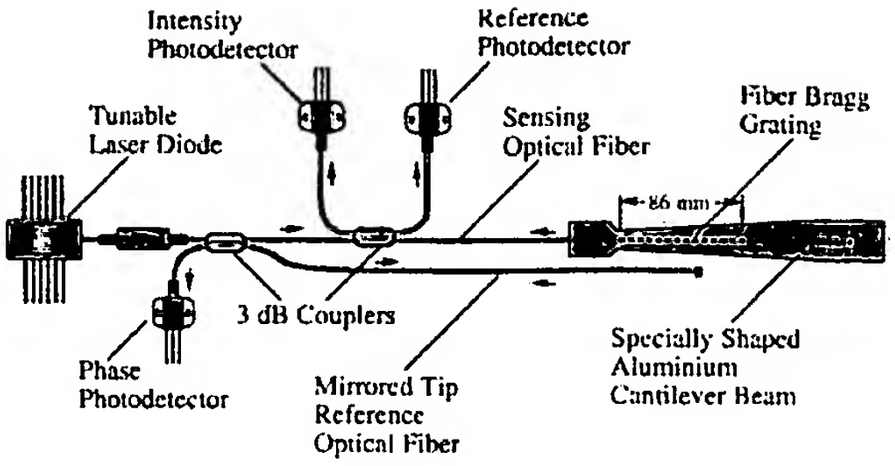

Figure 1. Schematic of experimental arrangement used to acquire both the intensity and phase reflected spectra from an extended strain-chirped fiber optic Bragg grating.

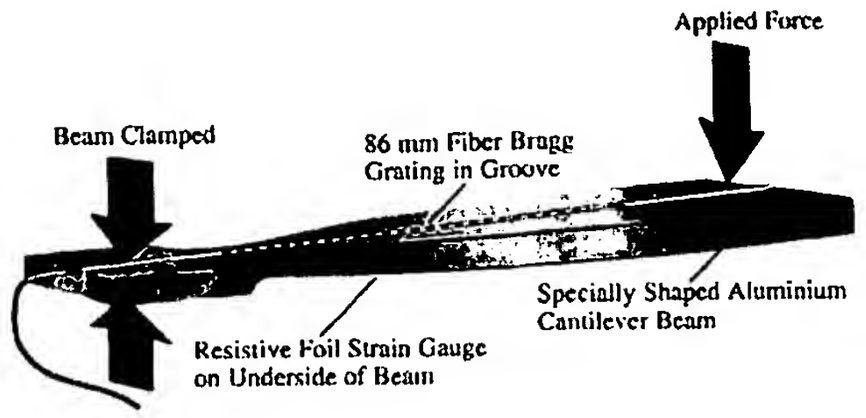

Figure 2. Specially shaped aluminum cantilever beam instrumented with an 86 mm long fiber optic Bragg grating sensor embedded within a fine axial groove cut into the beam.

Under these circumstances the inverse Fourier transform, equation (9), takes the form

$$\kappa(z)\,e^{i\phi(z)} = -\frac{i2n_0}{\lambda_0^2}\int_{-\infty}^{\infty}\sqrt{R(\Delta\lambda)}\,e^{-i\psi(\Delta\lambda)} \times \exp\left(-i4\pi n_0 z\Delta\lambda/\lambda_0^2\right)d(\Delta\lambda). \quad (12)$$

Using equation (12) and the experimental intensity and phase spectra we can compute both the amplitude $\kappa(z)$ and the argument $\phi(z)$ of the complex coupling coefficient. The former describes the axial variation in the coupling coefficient along the grating. The relation between $\phi(z)$ and the strain distribution, $\varepsilon(z)$, is given in equation (5) and can be put in the form

$$\varepsilon(z) = -\frac{\Lambda_0}{2\pi G_f}\frac{d\phi(z)}{dz}. \quad (13)$$

We see that the strain profile $\varepsilon(z)$ can be derived from the measured intensity and phase spectra of the grating using the inverse Fourier transform as given in equation (13). Note that for the sake of brevity we shall use $R(\lambda)$ and $\psi(\lambda)$ in place of $R(\Delta\lambda)$ and $\psi(\Delta\lambda)$ in the remainder of this paper.

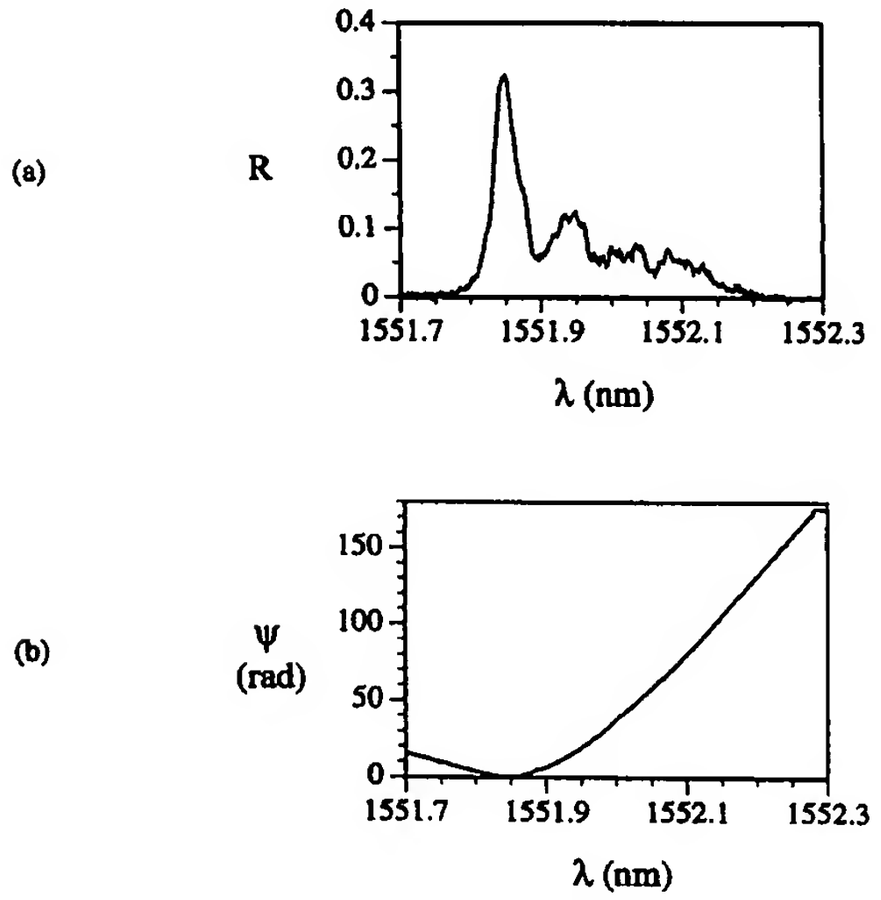

Figure 3. Measured (*a*) intensity spectrum $R(\lambda)$ and (*b*) phase spectrum $\psi(\lambda)$ for cantilever beam loaded to the resistive foil reading of 280 $\mu\varepsilon$.

3. Experimental Fourier transform distributed strain sensing

To date we have undertaken one preliminary experiment to test the new Fourier transform method of determining the arbitrary strain profile imposed upon a fiber Bragg grating. The experimental arrangement for acquiring the intensity and phase spectra, $R(\lambda)$ and $\psi(\lambda)$ respectively, is schematically depicted in figure 1. The semiconductor tunable laser operating at about 1552 nm scans approximately 2 nm wavelength interval that is sufficient to cover the reflection spectrum (intensity and phase) of the fiber Bragg grating. The laser power launched through the optical fiber at the grating is monitored by photodetector PD1 as a function of wavelength. Photodetector PD2 monitors the light reflected from the grating as a function of wavelength.

The ratio of the two signals from PD1 and PD2 as a function of wavelength is essentially proportional to $R(\lambda)$. A calibration of the system, accounting for the various non-common losses and the different spectral responses of the two photodetectors, permits $R(\lambda)$ to be determined. A third photodetector PD3 and a Michelson interferometric arrangement was established in order to monitor the phase spectrum $\psi(\lambda)$. In this first experiment a second coupler

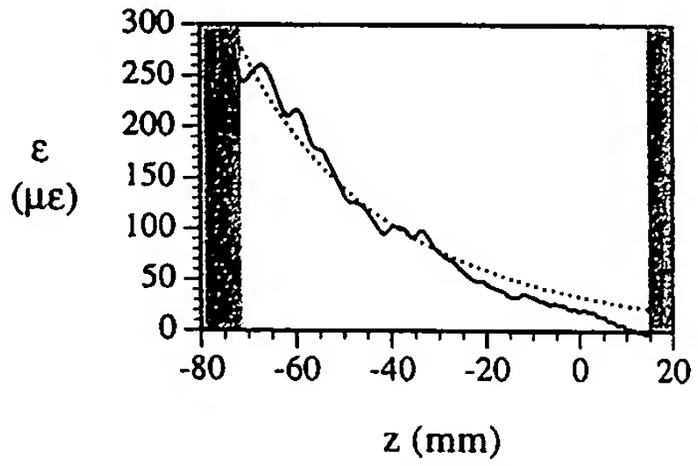

Figure 4. Comparison of strain profile along the grating as predicted by pure beam bending theory (dotted curve), and Fourier transform of intensity and phase spectra presented in figure 3 (full curve).

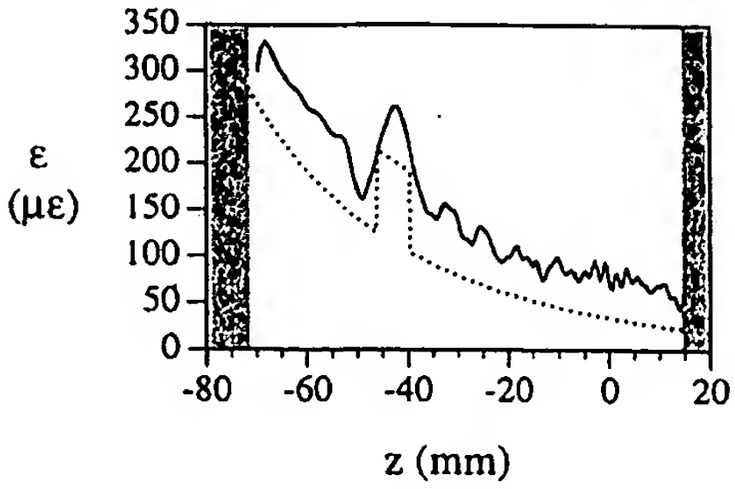

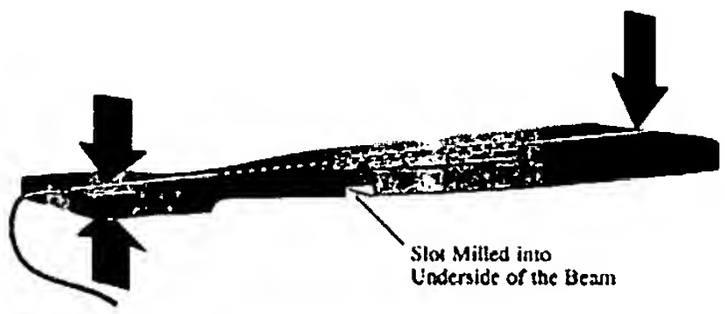

Figure 5. (top) Comparison of strain profile along the grating as predicted by pure beam bending theory (dotted curve) and Fourier transform of intensity and phase spectra (full curve) for beam with slot milled into beam (see bottom) and then loaded again to roughly 280 $\mu\varepsilon$ on the resistive foil gage.

and a second optical fiber with a mirrored end was used for this purpose. A Pentium PC was set up to control the laser wavelength and collect the data from the three photodetectors.

An 86 mm long fiber optic Bragg grating was epoxied into a small groove cut into the top of a specially shaped aluminum cantilever beam (figure 2). The beam was clamped at one end and a force applied at the other end. The groove technique tends to avoid the creation of unknown strains that can accompany surface bonding (LeBlanc *et al* 1994). A small resistive foil strain gage was adhered to the underside of the beam, directly beneath the near end of the fiber grating. Figure 3 displays the measured intensity and phase spectra, $R(\lambda)$ and $\psi(\lambda)$, recorded for one loading of the beam. The resistive foil gage registered a strain at the near end of the grating of about 280 $\mu\varepsilon$ for this loading. The computed strain profile based on pure beam bending theory is shown as the dotted curve in figure 4, while the full curve represents the strain profile as deduced by the Fourier transform method from the intensity and phase spectra. Although the experimental curve fits the theoretical curve reasonably well, for an initial experiment, there is considerable noise in the data. Some of the deviations from the smooth theoretical curve could be real and attributed to imperfections in the grating, or non-uniformity in the bonding of the grating to its host structure.

As a first step to ascertaining the spatial resolution of this sensor and verifying that the Fourier transform method overcomes the monotonic limitation of the individual intensity spectrum (LeBlanc *et al* 1996) and phase spectrum approaches (Huang *et al* 1996) a small slot was milled into the beam and the experiment repeated (Huang *et al* 1997). The dotted curve in figure 5(*a*) provides an initial estimate of the strain profile for the loaded beam with the slot, while the full curve portrays the strain profile predicted by the Fourier transform method. There are several observations to be made: the act of milling the beam seems, according to the experimental curve in figure 5, to have produced a residual strain bias; there also appears to be a local region of compression on the high tensile strain side of the slot, and the noise level seems to have been increased. In spite of these problems there is clear evidence that the predicted strain step was detected at the correct location, with about the right spatial extent, and a peak that is approximately correct when allowance is made for the general strain offset produced by the milling. Clearly much research and development will be needed before this new sensing modality can find general application, but at least the concept has been validated.

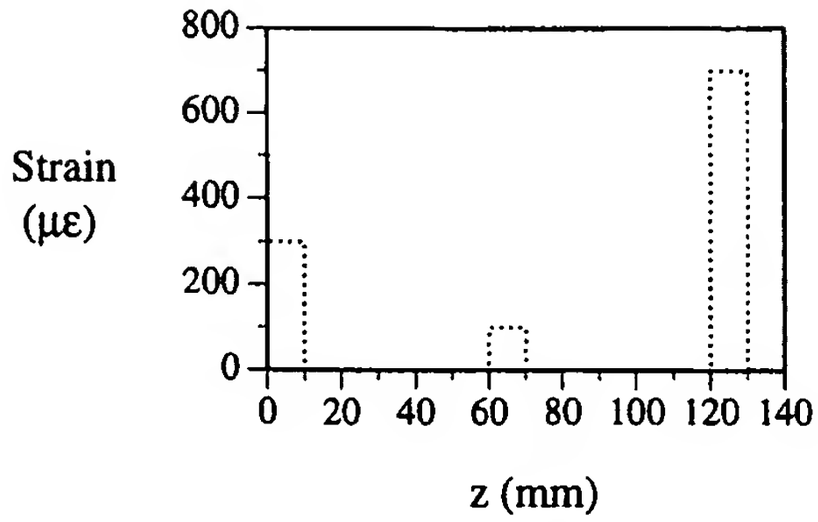

Figure 6. Assumed strain profile imposed on three FBG sensors located along an optical fiber.

4. Fourier transform serial multiplexed fiber Bragg grating sensors

Since a string of Bragg gratings along an optical fiber can be thought of as a Bragg grating with sections of zero reflectivity between the grating elements it is reasonable to anticipate that the Fourier transform approach might alas be used to evaluate the strain distribution from such a string of gratings. This represents a novel method of serial multiplexing a linear array of FBG strain sensors without recourse to the wide spectral width source required for wavelength division multiplexing or the fast pulse optoelectronics of time division multiplexing.

We have tested this concept first through computer simulation. In figure 6 we present the strain field to which we assume three FBG sensors in a string along an optical fiber are subject. The three intensity reflection spectra concomitant with this strain distribution are presented in figure 7, and the comparison between the expected strain readings according to the simulation and the input strain distribution is portrayed in figure 8. We can see that there is good agreement if one ignores the small oscillatory signals in the vicinity of the grating ends. We suspect that these oscillatory signals can be attributed to the finite spectral resolution of the system. It should be noted, however,

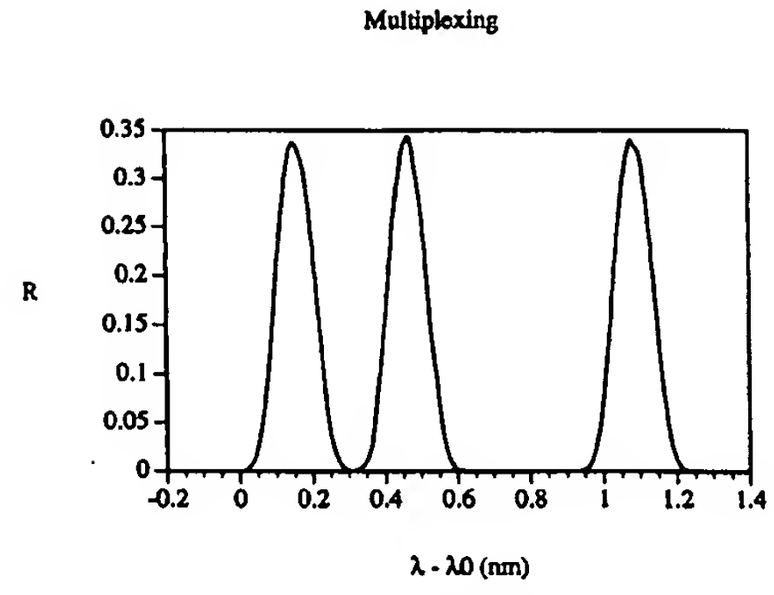

Figure 7. Computed intensity spectra reflected from three strained FBG sensors.

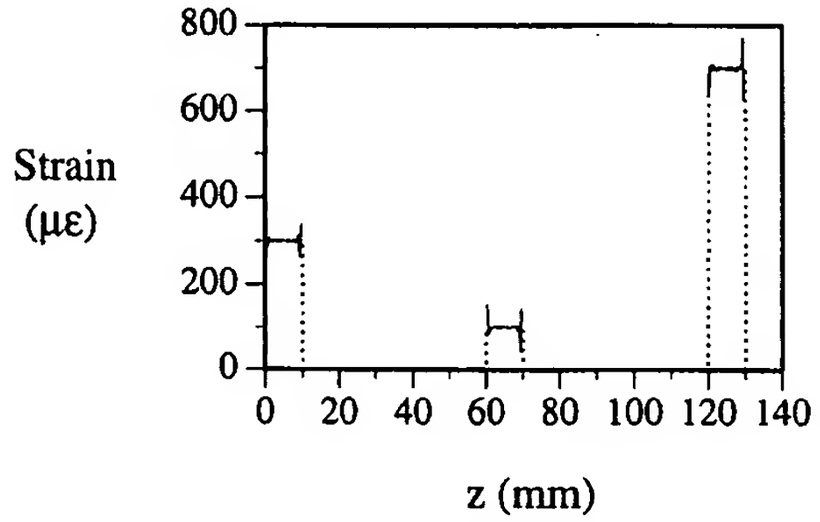

Figure 8. Comparison of imposed and Fourier transform calculated strains for the three FBG sensors.

that the Fourier transform analysis generates large false oscillatory signals in regions of zero reflection, i.e. where no grating exists. Since we know no light originates from such regions of the optical fiber we have omitted them in figure 8. More complete use of the Fourier transform information provides a means of checking where zero reflection arises and this could be incorporated into the computer program to avoid the appearance of such false data in the strain profile.

We have undertaken an initial experiment to test this novel multiplexing scheme. We bonded an optical fiber containing three short FBGs to the same specially shaped cantilever beam (prior to it being milled) as we used for the distributed sensing experiment. We also used the same tunable laser and the same intensity and phase spectrum measurement system, clearly demonstrating the universality of this demodulation system. Figure 9(*a*) displays the overlapped intensity spectrum of the three Bragg gratings when the beam was unloaded. The spectrum is degenerate and complex in nature resulting from interference between the three FBGs. As can be seen in figure 9(*b*), loading of the beam results in the removal of this spectral degeneracy and a separation of the spectra from the three FBGs.

The strain profile estimated from beam bending theory for the loaded beam is presented as the broken curve in figure 10. Superposed on this curve are the three strain profiles calculated for each of the three FBGs from the Fourier transform of their intensity and phase spectra. As can be seen, each sensor provides a part of the overall strain profile and although the trend is correct, clearly the precision of this technique needs to be improved. It is worth pointing out that there is a striking similarity between the deviation of these results from that predicted by the simple beam theory as was observed with the single extended FBG sensor (compare figures 4 and 10). This similarity in the strain profiles measured by three separate multiplexed gratings and the single extended grating suggests that the deviation from the simple beam theory prediction has some physical validity and may be due to some imperfection in the beam.

This Fourier transform approach to reading a linear array of FBGs is limited to lengths of a few meters due to the high frequencies involved in the intensity and phase spectral measurements. Nevertheless, this extends the range over which strain profiles can be measured from the limits of a single extended grating, which is probably limited to about 10 cm (before the cost becomes prohibitive) to a few meters which could satisfy most practical needs. It should be noted that this distributed strain sensing technique avoids the need for large bandwidth sources and a set of gratings with different reference wavelengths, as required for WDM. It also avoids the high cost of high-resolution OTDR needed by the TDM approach to evaluating strain profile with a string of gratings.

As we shall show in the next section, a similar type of measurement can be undertaken over much larger distances if the intensity and phase wavelength modulation arises from interference between relatively closely spaced FBGs rather than between each FBG in the array and a single reference mirror.

5. Excess strain localization for large linear sensor arrays

There are certain physical situations that require some indication of where excess loading is occurring along a large structure. A good example would be a pipeline that is subject to possible ground movement. In such applications it is important to not only detect when excess strain arises along the structure but also to pinpoint where this loading occurs. The ability to write many FBG sensors along the length of an optical fiber makes this technology very attractive for this application. Indeed, the ability to readily multiplex linear arrays of FBG sensors represents one of the major advantages of this technology over other strain sensing technology. For large structures where it is important to detect the onset of excess loading, a string of FBG strain sensors would seem to be ideal as all the FBG sensors could be made to have roughly the same reference wavelength making it fairly easy to detect the spectral walk-off of one (or more) sensors due to the development of excess strain at some location. The only problem is to then identify which FBG sensor is subject to this excess strain. Conventional thinking would suggest either WDM or TDM for this task. Unfortunately, the former would require a source with considerable bandwidth if many FBG sensors are to be interrogated, while the latter requires short-pulse optoelectronic technology, which is very expensive.

(a)

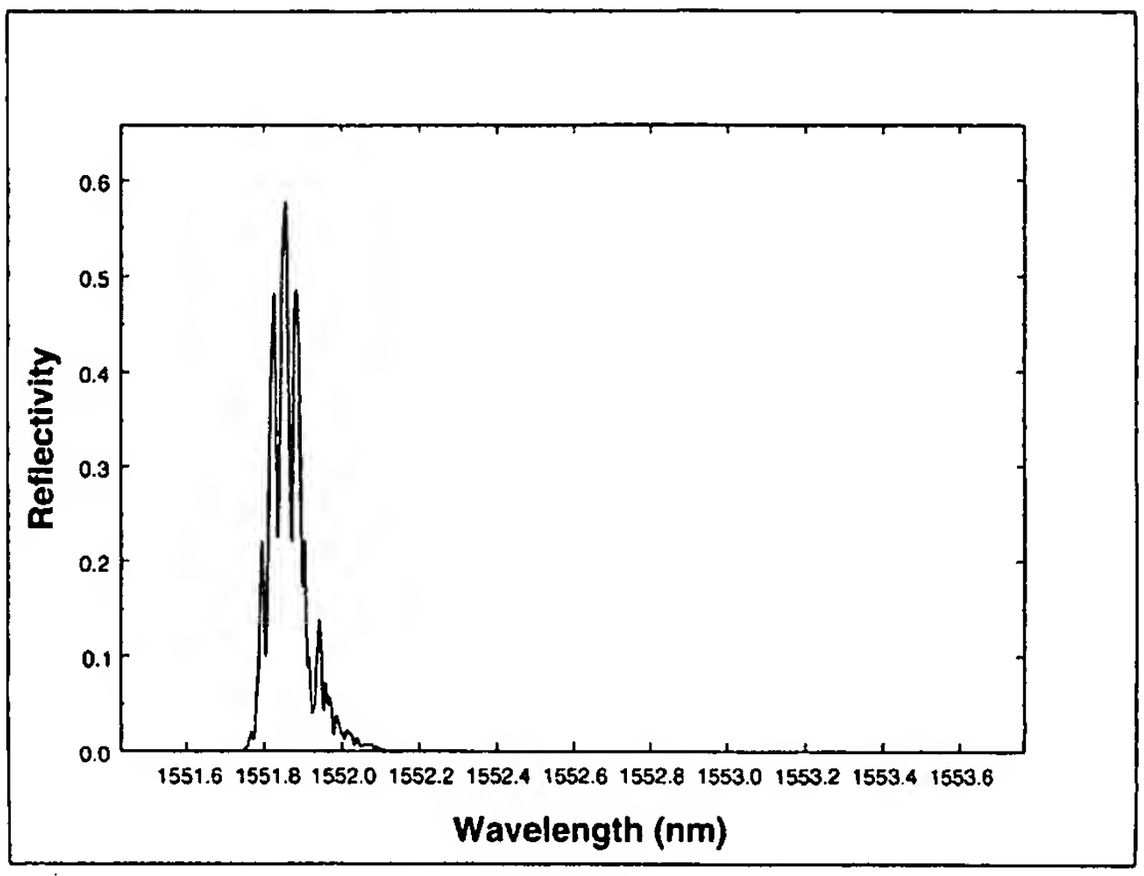

(b)

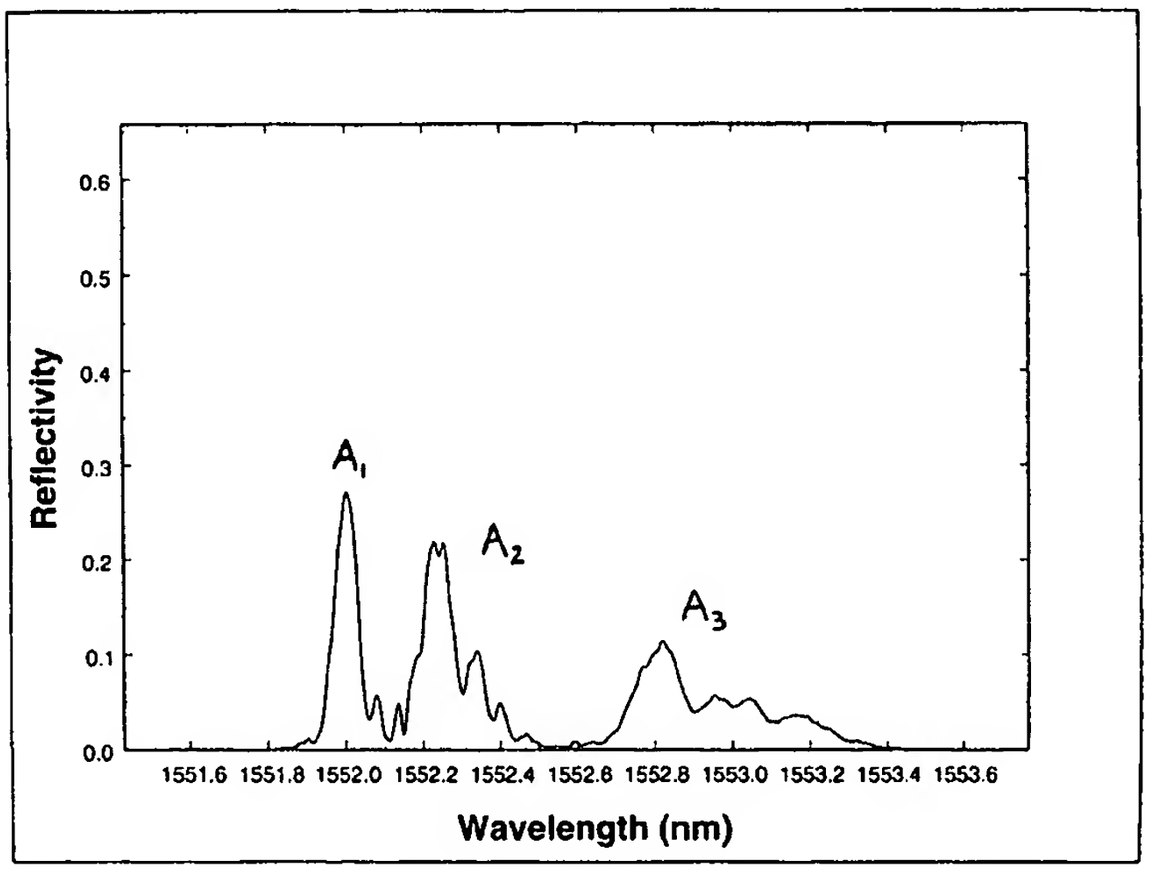

Figure 9. Intensity spectrum for three FBG sensors spread out along the single optical fiber bonded to the specially shaped beam, (*a*) prior to loading and (*b*) after the beam is loaded. The spectrum of the FBG subject to greatest strain gradient is indicated as A_1, while A_3 corresponds to the FBG subject to the minimum strain gradient.

Although we have shown that a tunable laser combined with Fourier transform analysis can be used for serial multiplexing, for large structures this requires a very narrow bandwidth laser in order that its coherence length can span the separation between the furthermost FBG and the reference mirror. For applications like pipelines where the structure could be hundreds of meters in length this approach is not practical. Furthermore, spectral measurements over distances of more than a few meters lead to very high frequencies that are beyond the spectral resolution likely to be attained in practice. However, we have applied the Fourier transform concept in a novel manner to overcome this limitation.

We have shown that if pairs of FBGs are used along an optical fiber—each pair having a slightly different separation—then Fourier transform analysis can be used to identify which pair of FBGs is subject to excess strain. If $f(\lambda)$ describes the reflection (or transmission) intensity spectrum for a given pair of FBGs, acquired by scanning the laser wavelength over the spectral interval (λ_0, $\lambda_0 + \Delta\lambda$), then the corresponding frequency (of wavelength oscillations) spectrum for this pair of FBGs can be derived from the Fourier transform of their intensity spectrum, $f(\lambda)$:

$$F\left(\frac{1}{\delta\lambda}\right) \approx \int_{\lambda_0}^{\lambda_0+\Delta\lambda} f(\lambda)\, e^{-i2\pi\lambda/\delta\lambda}\, d\lambda \qquad (14)$$

where the frequency of wavelength oscillations in the intensity spectrum corresponds to the inverse of the wavelength separation of the Fabry–Pérot modes formed

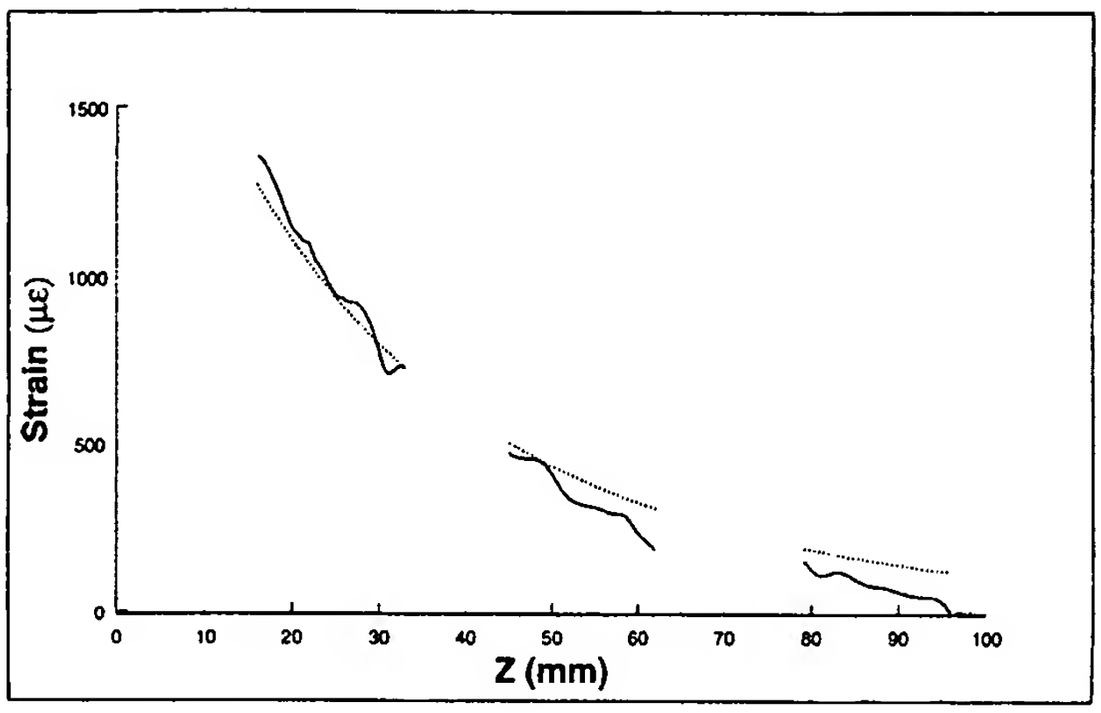

Figure 10. Comparison of strain profile along beam, as calculated according to simple beam bending theory (broken curve), and as obtained from the intensity and phase spectra using Fourier transform analysis (full curve).

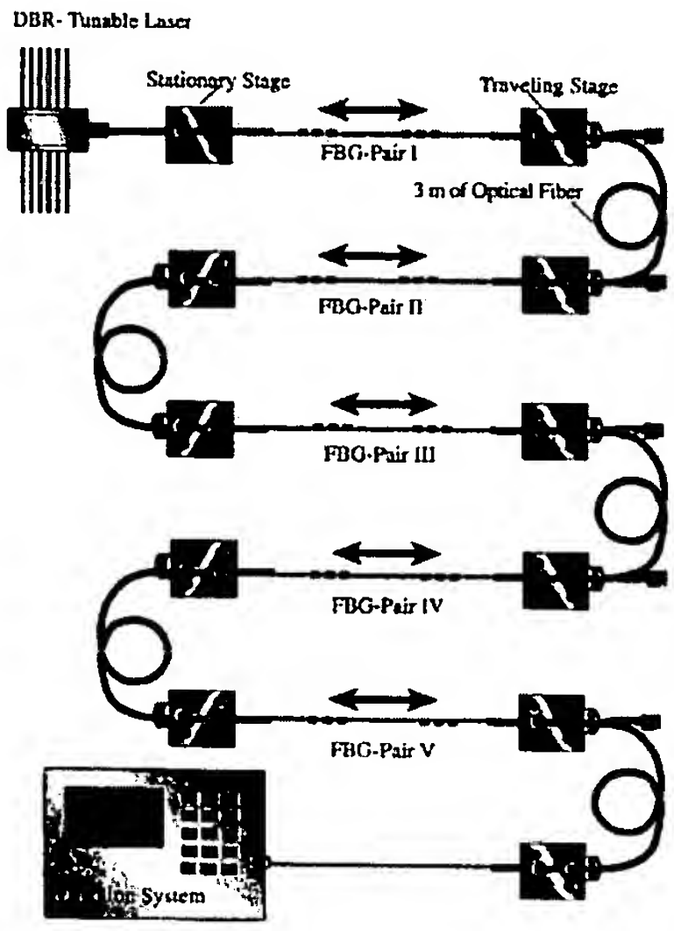

Figure 11. Schematic illustration of the experimental arrangement used to test the FBG pair sensor identification concept.

by the pair of FBGs:

$$\delta\lambda = \frac{\lambda^2}{2nL}. \tag{15}$$

Since $\delta\lambda$ is inversely proportional to the Fabry–Pérot cavity length, L, we see that the Fourier transform of the intensity spectrum gives directly the separation of the FBG pair.

A schematic of the experimental arrangement for a preliminary test of this concept is presented as figure 11. Five pairs of FBGs were produced in Ge-doped photosensitive optical fiber with measured grating pair separations plus penetration depths (i.e. Fabry–Pérot cavity lengths) of $L_I = 9.3$ cm, $L_{II} = 10.0$ cm, $L_{III} = 11.1$ cm, $L_{IV} = 11.9$ cm and $L_V = 12.5$ cm. Each grating was about 1 cm long and each pair of gratings was separated from its neighbours by approximately 3 m of Corning SMF-28 optical fiber. This 3 m of fiber loop ensured that each FBG pair was out of coherence with the adjacent FBG pair so that interference was restricted to the pairs of FBGs. Each grating pair is subject to its own strain state as each segment of optical fiber containing a grating pair is bonded at one end to a stationary block while the other end is bonded to a travelling stage controlled by a micrometer (figure 11).

The reflection and transmission spectra of five pairs of FBGs are displayed in figure 12, when a strain of about 380 $\mu\varepsilon$ is applied to all of the FBGs. The spectral walk-of (as seen in transmission) for the reflection spectrum of FBG pairs, I, II and IV, when a strain of approximately 380 $\mu\varepsilon$ is applied to each grating pair in turn, can be seen in figure 13. Although it is not possible to tell which FBG pair had been stressed from the reflection spectra, the Fourier transform of the wavelength displaced reflection spectrum indicates clearly which pair of FBGs has been subject to excess loading (see figure 14). Each FBG pair can be seen to have a distinctive frequency spike in the Fourier transform frequency spectrum corresponding to the resonance frequency of its Fabry–Pérot cavity length.

Even though these experiments are preliminary in nature they clearly suggest that the technique is worthy of further consideration. We have observed that in our experiments a strain of about 60 $\mu\varepsilon$ applied to one FBG sensor pair appears to be adequate to separate its spectrum from the composite spectrum of the remaining FBG pairs. Furthermore, a difference of just 1 cm in the separation of the two gratings constituting a FBG pair is sufficient for the Fourier transform analysis to identify which FBG pair is involved. It may well be possible to greatly improve on these figures with a less noisy laser and a more detailed study of this approach.

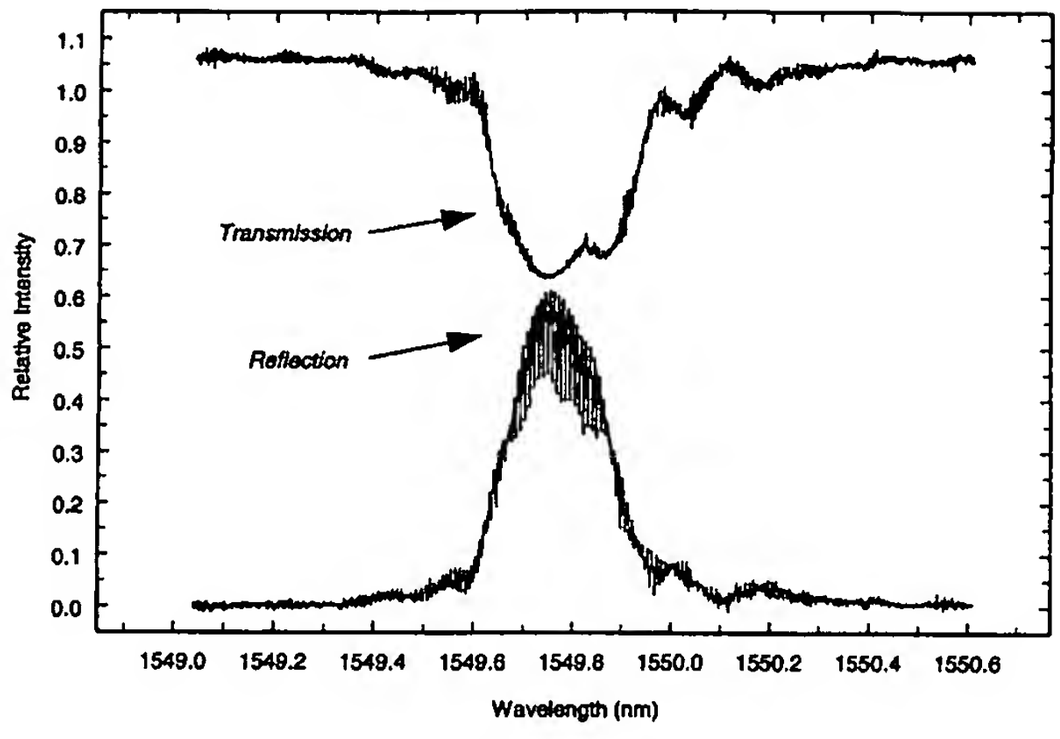

Figure 12. Superposition of the reflected and transmitted spectra from the set of five pairs of FBGs with no applied strain.

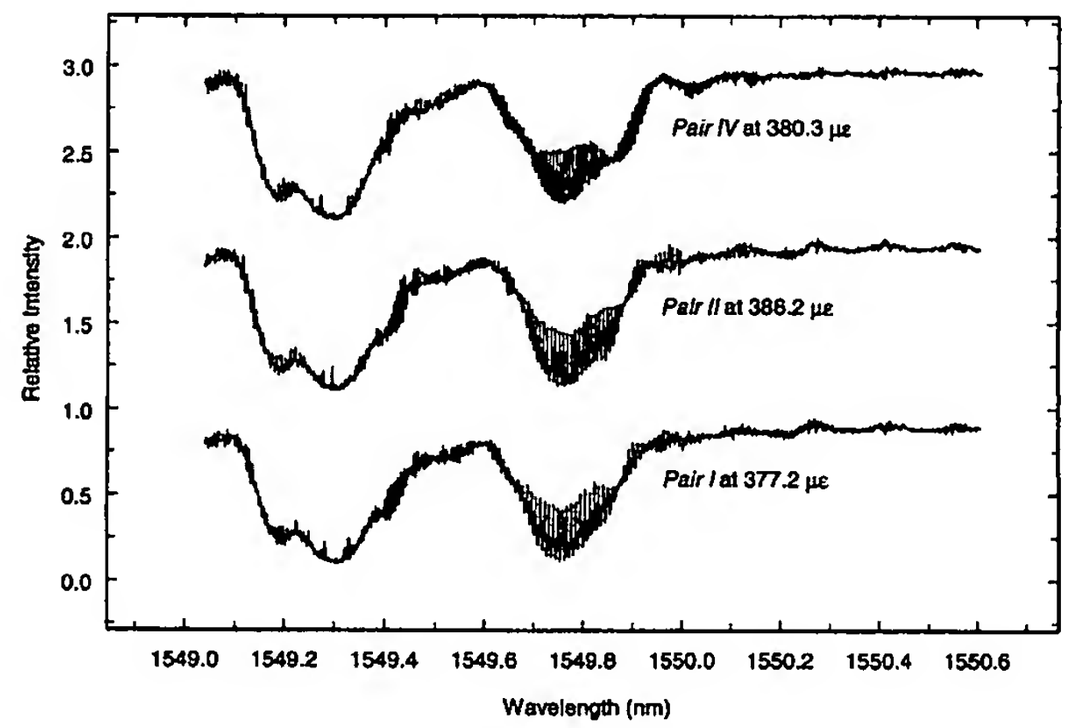

Figure 13. Three transmission spectra for the set of five pairs of FBGs corresponding to FBG pairs I, II and IV respectively being loaded to about 380 $\mu\varepsilon$.

6. Tunable laser long gage fiber optic stain sensor

A fiber optic strain sensor with an arbitrary gage length can be made by writing two FBGs in an optical fiber with a separation equal to the desired gage length. To ensure good spectral overlap between these two gratings it is necessary to make them as broadband as possible. Even so there will be restrictions on the difference in the strain and temperature at the two grating locations. One application for which this long gage Fabry–Pérot sensor is particularly well suited is the measurement of hoop stress in columns. This type of monitoring could be used to track the increase of pressure experienced by advanced composite material repair wraps due to continuing corrosion of the steel within these concrete columns. This monitoring technology could also provide valuable information on the status of columns subjected to earthquakes. In all of these types of hoop-stress monitoring application, the two gratings can be located in close proximity to each other thereby ensuring little difference in their strain and temperature.

The experimental arrangement for the long gage Fabry–Pérot strain sensor is schematically illustrated in figure 15. It can be shown (Fan *et al* 1997) for this configuration that scanning the laser over a spectral interval, $\Delta\lambda$, will result in a phase change recorded by the photodetector, PD1, as an intensity change resulting from interference between the light reflected from the sensing Fabry–Pérot interferometer and that reflected from the reference Michelson interferometer. With low-pass filtering we can extract the component of the phase change, $\Delta\phi$, that is directly related to the path imbalance between the two interferometers. The ratio of $\Delta\phi$ and $\Delta\lambda$ is, to first order, directly proportional to the difference between the Fabry–Pérot sensing gage length, L_S, and the length of the reference Michelson interferometer, L_R:

$$\Delta\phi/\Delta\lambda = 4\pi n(L_S - L_R)/\lambda^2. \qquad (16)$$

Preliminary experimental tests of this approach have been described elsewhere (Fan *et al* 1997). The elongation of a

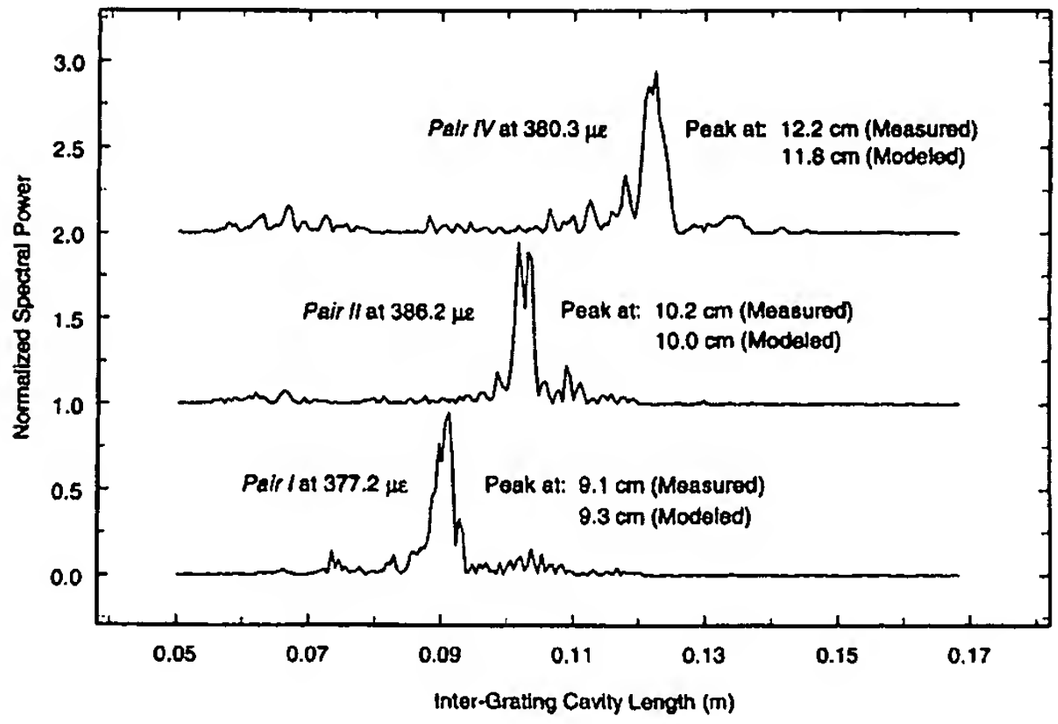

Figure 14. Fabry–Pérot cavity length identification by means of Fourier transform analysis for the three FBG pairs loaded in turn to about 380 $\mu\varepsilon$.

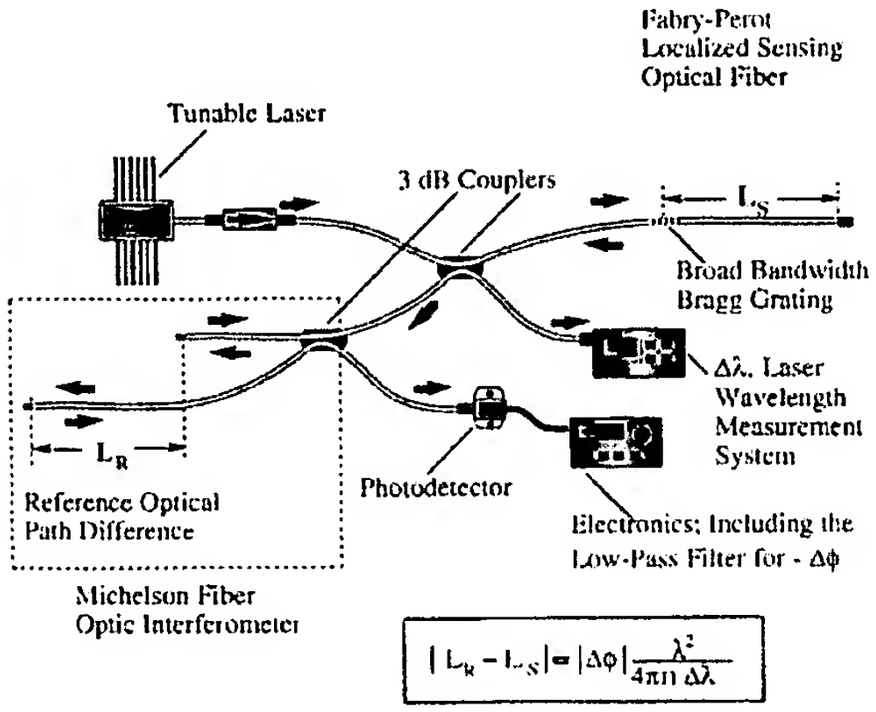

Figure 15. Schematic of experimental arrangement for testing the tunable laser demodulation of a long gage Fabry–Pérot fiber optic strain sensor.

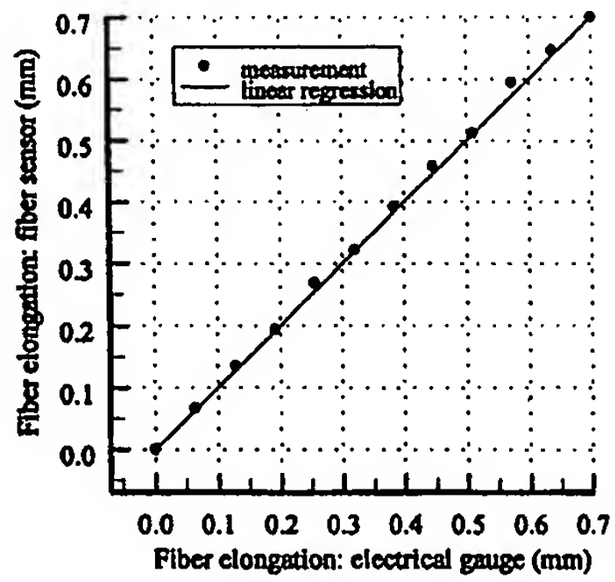

Figure 16. Linear variation of elongation as measured by the localized long gage fiber optic strain sensor and extrapolated from the resistive foil gage.

0.65 m Lexan test beam, as measured with this fiber optic sensor and compared with a conventional foil strain gage is presented in figure 16. It is sufficient to note here that again a tunable laser demodulation scheme is involved as with the multiplexed and distributed sensing systems described above.

7. Fiber Bragg grating universal demodulation system

As indicated above, we have recently gained an appreciation for some of the generic features that would lead to a fiber optic Bragg grating universal demodulation system. These are schematically portrayed in figure 17. At the heart of this system is a tunable laser and an isolator. Where parallel multiplexing is required a $(1 \times n)$ integrated optic splitter could be used to distribute the laser radiation amongst the 'n' sensing optical fibers. In figure 17, 'n' was taken to be 4. Each sensing optical fiber could contain a single FBG sensor, a linear array of FBG sensors, a long gage sensor, or an extended FBG to serve as a distributed strain sensor. What makes this demodulation approach so versatile is the detection module (DM) that fits between the $(1 \times n)$ splitter and each sensing optical fiber. Each DM has at least a pair of low-insertion-loss and low-reflection connectors, one for interfacing to the $(1 \times n)$ splitter, and the other for interfacing to the sensing optical fiber.

For a single FBG sensor the DM is very simple and comprises a pair of photodetectors and a 3 dB coupler as shown in figure 18(a). One photodetector, PD1, is used to monitor the optical power reflected from the FBG, while the second, PD2, is used to measure the laser power sent to the FBG and serves as a reference. The wavelength of the laser during scans could be monitored with a pair of detectors having some form of differential wavelength dependence (Measures *et al* 1992). We have recently demonstrated how this could be accomplished using a quantum well electroabsorption device (Coroy and Measures 1996) that could be mounted very close to the laser.

For each of the multiplexed and distributed sensing

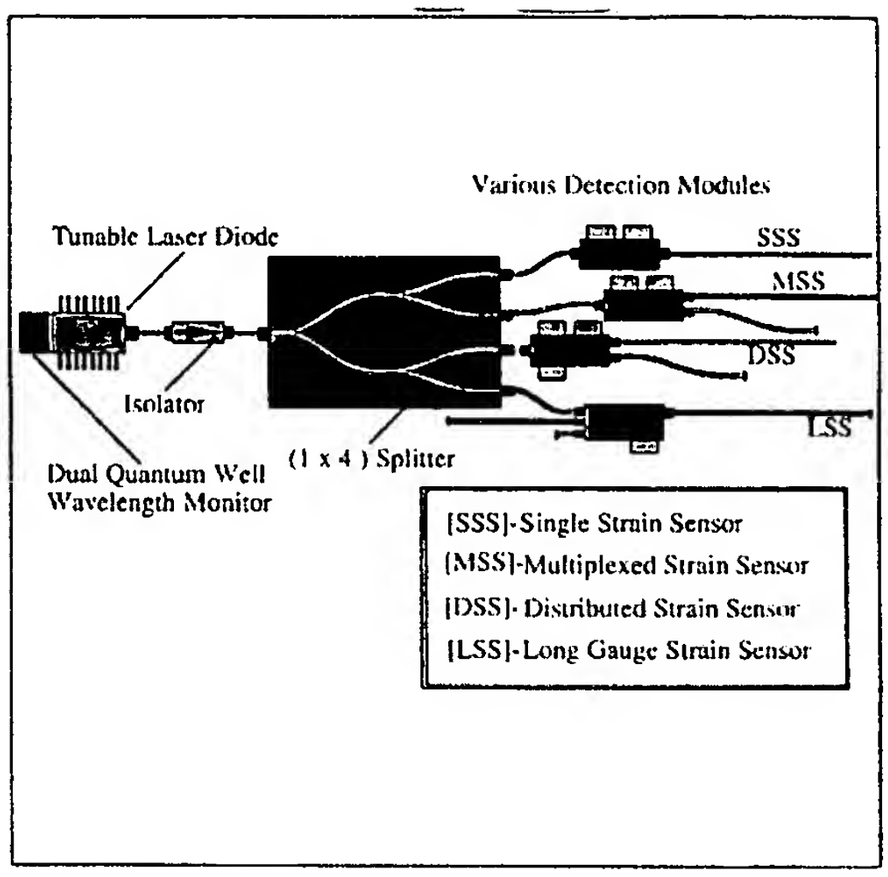

Figure 17. Schematic illustration of the generic features of a 'universal' FBG sensor demodulation system capable of undertaking short and long gage sensing as well as multiplexed and distributed strain sensing.

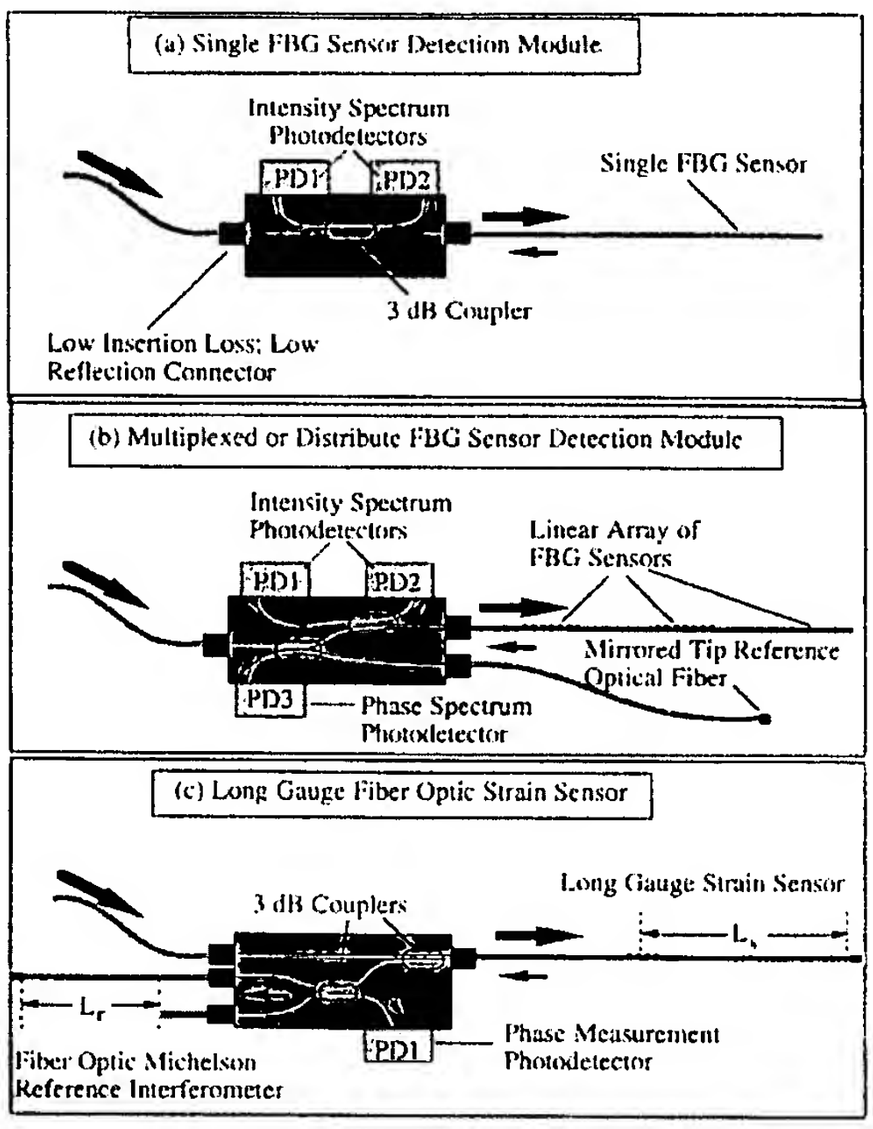

Figure 18. Three types of detection modules, DMs: (*a*) for single FBG short gage strain sensor; (*b*) for extended FBG distributed strain sensor, or linear array of short FBG sensors; (*c*) localized long gage strain sensor.

modalities there is a linear array of FBG sensors or an extended FBG distributed sensor; the DM contains three photodetectors and two couplers as shown in figure 18(*b*). In this case two of the photodetectors, PD1 and PD2, are

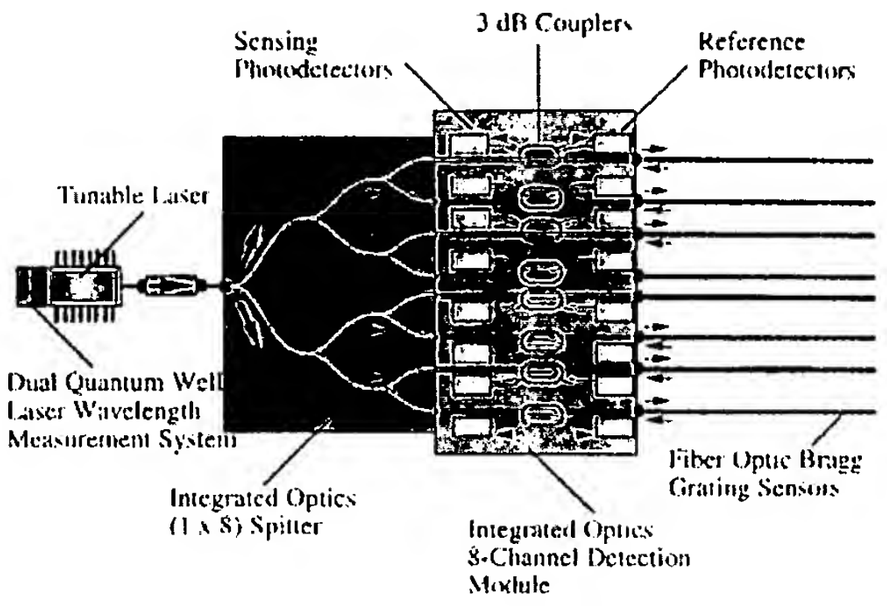

Figure 19. Schematic illustration of an eight-channel parallel multiplexed short gage FBG strain sensing system based on an integrated optic (1 × 8) splitter and an eight-channel integrated optoelectronic detection module.

used to extract the intensity spectrum, $R(\lambda)$, while the third, PD3, is used to measure the phase spectrum $\phi(\lambda)$. This type of DM also has a third low-insertion-loss and low-reflection connector for the mirrored tip reference optical fiber of the Michelson interferometer. In the case of the long gage length sensor the DM would comprise two couplers and a single photodetector connected through a low-insertion-loss and low-reflection connector to a reference Michelson interferometer as indicated in figure 18(*c*).

The beauty of this system is its modular form that would allow great flexibility and adaptability. The tunable laser unit can be used on certain occasions to work with a $(1 \times n)$ splitter and a set of 'n' simple DMs to interrogate 'n' single FBG sensors, while on other occasions it could be used with say a $(1 \times n)$ splitter and a set of 'n' interferometric DMs to interrogate a mix of distributed, long gage and multiplexed FBG sensors. Eventually, if there is sufficient demand, the tunable laser and its wavelength measurement system, the splitter, the couplers and the set of photodetectors, could be formed into optoelectronic integrated circuit modules. This would greatly reduce the cost of the system and avoid much of the pigtailing. It would also lead to a very compact and rugged system with reduced power requirements. Figure 19 schematically illustrates an eight-channel short gage fiber optic Bragg grating sensing system made of optoelectronic integrated circuit modules.

8. Concluding remarks

Fiber optic Bragg gratings have a number of attractive features including an unrivaled structural measurement versatility. They can be used to measure both strain and temperature. FBGs can determine the strain at a point or evaluate the strain integrated over a long gage length, they can be serially multiplexed and they can be used to determine the strain profile along a structure with a spatial resolution of about 1 mm.

In this paper we propose that all these different strain measurements can be undertaken with a demodulation architecture that is equally versatile. At the heart of this universal demodulation system would be a tunable laser

diode. The modular form of the proposed demodulation system would make it possible to configure the optimum system for any mix of measurements.

We have developed a technique based on intensity and phase spectral measurements combined with Fourier transform analysis that permits truly distributed strain sensing of arbitrary strain profiles with a single extended fiber Bragg grating. We have also shown that this technique permits strain profiles to be measured over distances much greater than possible with a single FBG by using a string of such grating sensors. What makes this approach particularly attractive is that it permits a string of FBG sensors to be interrogated without recourse to the higher cost of WDM or TDM techniques.

We have also developed a novel approach for detecting and locating excess strain along a large (extending over tens to hundreds of meters in length) linear array of fiber Bragg grating strain sensors. This technique relies on using pairs of FBGs instead of individual gratings. Any pair of such FBGs subjected to sufficient strain to separate them from the reflection spectrum of the remaining FBG pairs can be identified by the cavity length of the Fabry–Pérot interferometer so formed through Fourier transform analysis.

Acknowledgments

Funding for this work was provided by the Natural Science and Engineering Research Council, the Intelligent Sensing for Innovative Structures Network of Centres of Excellence, and the Ontario Laser and Lightwave Research Centre. We would also like to acknowledge the outstanding help from Greg Fishbein, Ning Yao Fan and Michel LeBlanc from our laboratory and the help of Robin Tam from the Ontario Laser and Lightwave Research Centre.

References

Fan N Y, Huang S Y and Measures R M 1997 Localized long gage fiber optic strain sensors *Smart Mater. Struct.* submitted

Huang S Y, Ohn M and Measures R M 1996 Phase-based Bragg intragrating distributed strain sensor *Appl. Opt.* **35** 1135–42

——1997 Continuous arbitrary strain profile measurements with fiber Bragg gratings *Smart Mater. Struct.* submitted

Kersey A D, Berkoff T A and Morey W W 1992 High resolution fiber grating based strain sensor with interferometric wavelength shift detection *Electron. Lett.* **28** 236

——1993 Multiplexed fiber Bragg grating strain-sensor system with a fiber Fabry–Pérot wavelength filter *Opt. Lett.* **18** 1370–2

Kersey A D and Morey W W 1993 Multiplexed Bragg grating fiber–laser strain-sensor system with mode-locked interrogation *Electron. Lett.* **29** 236

Kogelnik H 1976 Filter response of nonuniform almost-periodic structures *Bell Syst. Tech. J.* **55** 109–26

LeBlanc M, Huang S, Ohn M M and Measures R M 1994 Tunable chirping of a fiber Bragg grating using a tapered cantilever beam *Electron. Lett.* **30** 2163

LeBlanc M, Huang S Y, Ohn M, Measures R M, Guemes A and Othonos A 1996 Distributed strain measurement by use of a fibre Bragg grating and reflection spectrum analysis *Opt. Lett.* **21** 1405–7

Measures R M, Melle S and Liu K 1992 Wavelength demodulated Bragg grating fiber optic sensing systems for addressing smart structure critical issues *Smart Mater. Struct.* **1** 36–44

Nellen P M, Bronnimann R, Sennhauser U, Askins C G and Putnam M A 1996 Strain measurements on concrete beam and carbon fiber cable with distributed optical fiber Bragg grating sensors *Opt. Eng.* **35** 2570–7